ACS APPLIED MATERIALS & INTERFACES

Research Article

www.acsami.org

Thermally Tailored Gradient Topography Surface on Elastomeric Thin Films

Sudeshna Roy,[†] Nandini Bhandaru,[†] Ritopa Das, G. Harikrishnan, and Rabibrata Mukherjee*

Instability and Soft Patterning Laboratory, Department of Chemical Engineering, Indian Institute of Technology Kharagpur 721302, India

Supporting Information

ABSTRACT: We report a simple method for creating a nanopatterned surface with continuous variation in feature height on an elastomeric thin film. The technique is based on imprinting the surface of a film of thermo-curable elastomer (Sylgard 184), which has continuous variation in cross-linking density introduced by means of differential heating. This results in variation of viscoelasticity across the length of the surface and the film exhibits differential partial relaxation after imprinting with a flexible stamp and subjecting it to an externally applied stress for a transient duration. An intrinsic perfect negative replica of the stamp pattern is initially created over the entire film surface as long as the external force remains active. After the external force is withdrawn, there is partial relaxation of the applied stresses, which is manifested as reduction in amplitude of the imprinted features. Due to the spatial viscoelasticity gradient, the extent of stress relaxation induced feature height reduction varies across the length of the film (L), resulting in a surface with a gradient topography with progressively varying feature heights (h_F). The steepness of the gradient can be controlled by varying the temperature gradient as well as the duration of precuring of the film prior to imprinting. The method has also been utilized for fabricating wettability gradient surfaces using a high aspect ratio biomimetic stamp. The use of a flexible stamp allows the technique to be extended for creating a gradient topography on nonplanar surfaces as well. We also show that the gradient surfaces with regular structures can be used in combinatorial studies related to pattern directed dewetting.

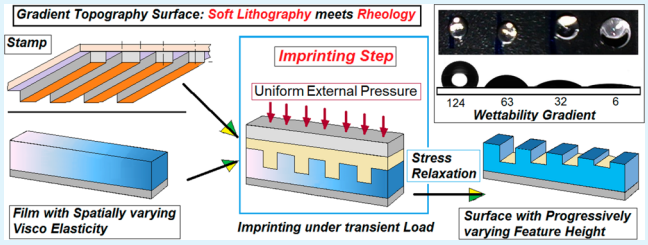

KEYWORDS: *topographic gradient, stress relaxation, viscoelasticity, hydrophobic, biomimetic, wettability gradient*

INTRODUCTION

Surfaces with continuous gradient in properties such as wettability, morphology, thickness, etc., are central to various important applications such as tissue morphing,[1] protein adsorption,[2] directional movement of cells and other macromolecules,[3,4] fabrication of optical intensity gradient materials,[5] various biomedical and sensor applications,[6,7] nanometrology,[8] etc. Gradient surfaces also find wide application in combinatorial studies related to wetting and dewetting, adhesion, friction, phase segregation, biocompatibility, etc.[9−13] An exciting observation on a wettability gradient surface is the gravity defying uphill movement of a liquid drop because of passive driving force originating from the imbalance in the horizontal component of surface tension along the contact line.[14−20]

Existing literature shows that gradations in surface patterns are most commonly created by either of the following two distinct approaches:[21] (1) directly adding a coating on to a substrate which has progressively varying surface property;[3,22−37] or (2) a pre-existing uniform coating is suitably modified to achieve the gradient properties.[8−12,38−46] To facilitate discussion and to highlight the novelty of the present work, we present a brief consistent review of the major techniques reported for fabricating gradient surfaces. Progressively varying the concentration of a deposited self-assembled monolayer (SAM) across the length of the film is the simplest way to obtain a gradient with continuous variation in surface energy. This is achieved by dip coating with variable withdrawal speed/immersion time.[22,23] Vapor phase diffusion-controlled deposition on a vertical substrate has also been used to fabricate surfaces with gradient properties, where the number density of the deposited molecules gradually reduce with increased vertical distance from the evaporating liquid solution.[14−16,24] Methods such as deposition under an electrochemical gradient,[25] soft lithographic technique along the lines of micro contact printing with varying contact time,[11,26] grafting of polymer brushes under a temperature gradient,[27] SPM-based techniques,[28] microfluidic techniques,[3] drop drying,[29] etc., have also been adopted for creating surfaces with gradient chemical properties. For fabricating surfaces with gradient topography, the method that is most widely used is based on the attachment of particles (nanoparticles/colloids) with progressively varying number density across the length of a surface.[30−34] A pre-existing chemical gradient greatly enhances the differential rate of particle attachment and therefore, a topographic gradient surface is often fabricated on such a template.[30,31] Another method that is widely used for fabricating gradient surfaces is flow coating, which can create films with

Received: January 9, 2014
Accepted: April 3, 2014
Published: April 3, 2014

   dx.doi.org/10.1021/am500163s | ACS Appl. Mater. Interfaces 2014, 6, 6579−6588

continuously varying thickness.[35] Flow coated block copolymer (BCP) films have been used for generating gradient topographies with features varying from micro- to nanoscale, as the lateral dimension of the phase segregated domains change continuously.[36,37]

Examples of the second approach includes gradual modification of a pre-existing uniform coating by different techniques such as gradient UV exposure,[8,11,12] controlled chemical etching,[10,38] controlled exposure to laser,[39] X-ray,[40] corona,[41] radio frequency (RF) discharge,[42] etc. Photolithography with custom-made masks having spatially varying feature dimension or number density of features has also been utilized.[17,19,43,44] However, fabrication of custom tailored photo masks with spatially varying feature dimensions/number density require elaborate nanofabrication facility. Cao et al. showed that a regular photo mask with uniform features can be used to generate a topographic gradient by placing an additional blocking mask just above the photoresist layer. Optical diffraction at the edges of the blocking mask during exposure generates a gradient in the intensity of light on the photoresist layer, which translates into gradient topography during development.[43] Zhang et al. explored the possibility of fabricating a topographic gradient by partially melting a self-assembled hexagonal closed packed array of colloidal Polystyrene particles by exposing it to a temperature gradient.[34] A combination of lithography and controlled chemical etching has been used to create a surface with combined topography and chemical composition gradient.[38] Several other approaches such as magnetolithography with magnetic particles,[45] self-organized wrinkling on surfaces,[46] etc., are examples of utilizing the second approach for the fabrication of gradient topography surfaces.

Careful scrutiny of the published literature reveals that most of the topographic gradient surfaces either have progressively varying feature dimension or varying number density along their length. However, fabricating a gradient topography surface where the feature height of the patterns varies continuously along the surface has rarely been reported.[47] Such a surface would be ideally suited as templates for combinatorial experiments, particularly in studies involving wetting, friction, and adhesion.[9−13] In this article, we report a simple method for fabricating a topographic gradient surface with progressively varying feature height across the length, whereas the lateral dimension, number density, and the periodicity of the imprinted patterns remain unaltered. Most importantly, the gradient is obtained using a single stamp with uniform features, and in a single step eliminating the need of a chemical gradient template. The method relies on initially creating a film that has coexisting gradients in both viscous and elastic modulii across the surface of a thermo curable elastomer layer. This is achieved by means of varying the rate of cross-linking reaction across the film surface, obtained by exposing the film to a gradient temperature field. The film with gradient visco elasticity is subsequently imprinted under a transient external force. The gradient in modulus results in varied stress relaxation upon removal of the applied external stress resulting in a topographic gradient surface. The steepness of the gradient surface can further be controlled by adjusting the magnitude of the temperature gradient and other related processing conditions. The approach is clearly distinct from an earlier work by Ding et al., where a Nano Imprinted film was exposed to a programmed temperature gradient to obtain progressively varying feature height.[47] Using a high aspect ratio biomimetic stamp replicated from natural lotus leaf, we successfully extend the method for fabricating wettability gradient surfaces exhibiting complete wetting at one end ($\theta_E < 5°$) to significant level of hydrophobicity on the other end ($\theta_E \approx 127°$). We also show that the proposed method can be utilized for creating a topographic gradient on a film coated on a nonplanar substrate, which to the best of our knowledge has been demonstrated for the first time.

We further utilized the gradient topography substrates with regular features for understanding how the feature height influences the dewetting pathway, morphology and ordering of thin polymer films directly spin-coated on them. Earlier studies on discrete samples with different feature height showed morphological transition with variation in substrate feature height.[48] However, the precise substrate height at which the regime cross overs take place could not be determined with accuracy. By performing combinatorial dewetting experiments on gradient topography substrates, we identify the critical feature height for a specific film thickness and geometry at which different regime cross overs take place and present a morphology phase map based on that. This study can act as a guide to obtain instability mediated ordered features based on pattern directed dewetting, which is gaining wide popularity as a viable non-lithographic mesopatterning technique.[49]

MATERIALS AND METHODS

Film Preparation. The gradients are created on films of Sylgard 184, a two part thermo curable Polydimethylsiloxane (PDMS) elastomer (Dow Corning, USA). In our experiments, the oligomer (part A) to the cross-linker (part B) concentration is maintained at 10:1 (v/v). The composition of Part A (as indicated by the product data sheet) oligomer is a combination of vinyl terminated siloxanes (dimethyl-vinyl terminated dimethylsiloxane) and tetra(trimethylsiloxy) silane. The curing agent (Part B) is a dimethyl, methyl hydrogen siloxane.[50] The films are dip coated from a solution in n−Hexane (HPLC grade, Merck India) on cleaned glass slides (50 mm × 25 mm) using a dip coater (Appex Instruments, India) at a constant withdrawal speed of 50 mm/min. Films of two different thicknesses are coated: ∼5 μm (dilution in solvent 1:10) and 20 μm (dilution 1:4). The films are air-dried for 20 min after coating, to allow evaporation of excess solvent. Some films of 5 μm thickness are coated on the outside surface of cleaned glass test tubes (12 mm OD, 80 mm long). The thickness of the coated films was estimated based on weight difference before and after coating the film, which is a standard technique for measuring the thickness of films with few micrometers thickness.[51]

Stamps for Patterning. Two types of stamps are used in this study. For quantifying the steepness of the gradients, patterns with regular features are necessary and for this purpose patterned aluminum foils stripped from commercially available optical discs such as CD, DVD, and Blue Ray discs (BRD) are used.[52,53] These foils have grating structure and are widely used as low-cost stamps for soft lithography. As the feature height of these foils are rather low (varies between 40 nm in a BRD to 120 nm in a CD foil), they have inadequate capacity to create patterns that exhibit structural superhydrophobicity in the Cassie state of wetting.[54] To overcome this limitation, we also used stamps with higher feature height to show the effectiveness of the current method in fabricating a wettability gradient. As an alternative to the expensive formal lithography facility, we used biomimetic stamps fabricated by replica molding of natural lotus leaves (Nelumbo Nucifera L.).[55] Lotus leaves have micro pillars on their surfaces (height ≈ 15 μm), which allows them to exhibit Cassie state of hydrophobicity. To fabricate a stamp out of a lotus leaf, first a negative replica of the leaf is made on a self-standing block (∼500 μm thick) of the elastomer by replica molding. After pouring the degassed prepolymer solution on a cleaned piece of the leaf, it is allowed to cross-link at room temperature (25 °C) for 48 h.[55] High-temperature annealing is avoided to prevent possible damage to the leaves and the structures thereon. The replica molded elastomeric block comprising of a random collection of holes is subsequently used as the stamp for creating the topographic gradient

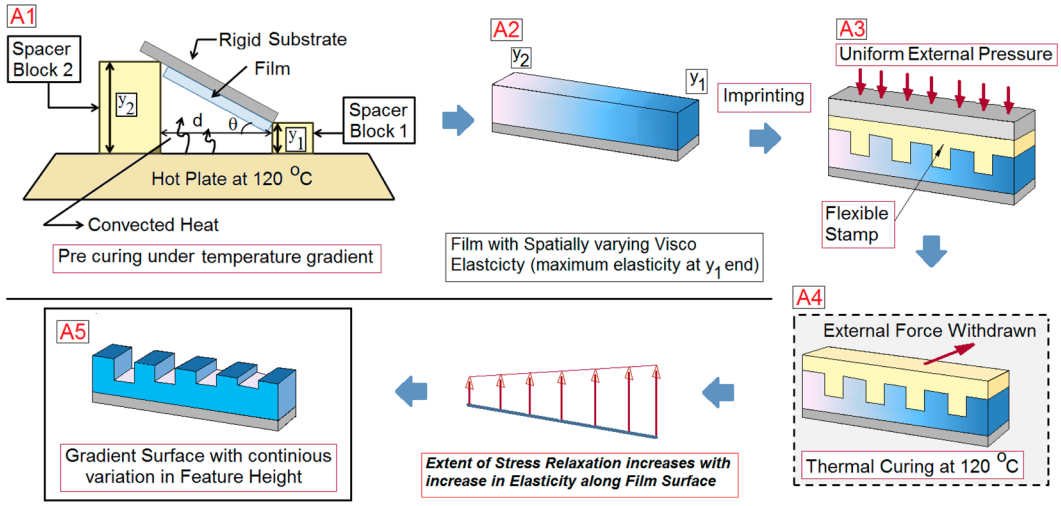

Figure 1. Schematic representation of the key steps of the method for generating topographically patterned surfaces with continuous variation in feature height, based on stress relaxation in a partially cross-linked viscoelastic thin film.

surface on the films. To prevent possible cohesive bonding between the stamp and the film during imprinting (as both are of the same material), the negative replica of the leaves are exposed to UV ozone (UVO) for 30 min in a UVO chamber (PSD Pro UV−O, Novascan, USA). UV irradiation at a wavelength of 184.9 nm dissociates molecular oxygen into atomic oxygen, which recombines with the molecular oxygen to produce ozone. The ozone further gets dissociated by the 253.7 nm UV−C irradiation resulting in the formation of atomic oxygen, which reacts with the siloxane group of the elastomer, forming a stiff oxide layer at the surface of the stamp.[51,55] The oxide layer prevents cohesive bonding between the stamp and the uncured film during the gradient fabrication step, and facilitates easy detachment after pattern replication. It is worth highlighting that upon double replication, the nanoscale secondary patterns on the lotus leaf are lost, which leads to slight reduction in the extent of hydrophobicity on the replicated Sylgard 184 surface (water contact angle 157°) as compared to a natural, fresh lotus leaf (162°). However, this in no way affects the generation of the wettability gradient surface.

Patterning Technique. For creating a gradient topography by the proposed method, it is essential to initially have a film that has spatially and progressively varying viscoelastic modulii across the length of the surface. For this, the dip coated and un-cross-linked film is first precured before imprinting by keeping it slanted over a hot plate (Tarsons, model 5060), by means of supporting it on two ceramic blocks of dissimilar heights (marked as spacer blocks), as shown in frame A1 of Figure 1. In all our experiments, the hot plate is preheated to 120 °C before placing the film on the spacer blocks. The experimental arrangement ensures that the distance between the heat source (hot plate) and the film surface progressively increases from y_1 at the lower end to y_2 at the top. This creates a continuous temperature variation across the film surface, which is measured using a non contact digital infrared thermometer (Metravi, MT-5). The precuring time (t_p) is so chosen that the film is always in a partially cross-linked state. In our experiments, t_p is varied between 1.5 and 30 min, as parts of the film closest to the hot plate started to cross-link completely for t_p > 30 min.

The precured films are subsequently imprinted with a flexible foil stamp (mass 5 g) placed conformally over the entire film surface. A uniformly distributed weight of 500 g is placed over the foil, which corresponds to an imprinting pressure of 2 KPa. On the basis of control experiments, we verified that the applied stress is adequate to form an intrinsic perfect negative replica of the stamp over the entire film surface. In actual experiments, the external pressure is withdrawn after applying it for 1 min only. The imprinted films along with the stamps are subsequently annealed in an air oven for 12 h at 120 °C for complete cross-linking of the film and making the patterns permanent. Once fully cross-linked, the patterns do not relax any further and the feature height remains unaltered, which was verified on the basis of control experiments, by scanning the same area again and again with an AFM over several (up to 15) days. The feature height variation for a zone with feature depth of 65 nm was found to be only ±0.7 nm, which confirms that the feature height does not change with time. A nearly identical protocol is followed for fabricating the gradient on the cylindrical tube, with additional low RPM rotation of the tube to ensure uniform radial preheating. An uniform pressure along the circumference of the cylindrical tube was ensured by rolling the tube coated with the partially cured film over the foil stamp at a constant velocity, which resulted in an adhesion between the film surface and the stamp.

Gradient Characterization. After complete cross-linking, the films are cooled to room temperature and the stamps are manually peeled off. The samples are characterized using an AFM (Agilent Technologies, model 5100) in intermittent contact mode, using a Silicon Cantilever (PPP-NCL, Nanosensors Inc. USA). The feature heights (h_F) are measured at five different locations on each sample. The points are identified as L_0 (film tip at the y_1 end), L_{13}, L_{25}, L_{37} (12.5, 25, and 37.5 mm away from the y_1 end, respectively) and L_{50} (y_2 end). Films patterned on curved surfaces are also scanned under the AFM following a specific sample mounting protocol described elsewhere.[56] The maximum feature height of the structures obtained with the biomimetic stamps is ∼14 μm, which is higher than the maximum Z range of the AFM scanner (∼7.5 μm) and are therefore investigated with an SEM (JSM 5800, JEOL, Japan) and a surface profilometer (Veeco, Dektac 150). The spatial variation in wettability is investigated using a contact angle Goniometer (Ramé-hart, USA, model −290 G1).

Rheological Characterization. The change in viscoelasticity during the cross-linking of Sylgard 184 films as a function of temperature is analyzed using a Rheometer with a cone and plate assembly (Anton Paar, Physica MCR 301, Austria, plate diameter: 25 mm, cone angle ∼2°, sample thickness ∼1 mm). For this purpose, bubble free Sylgard-184 prepolymer mixture is poured on to the Rheometer plate at room temperature and is subjected to oscillations at a constant angular frequency of 10 s^{-1} at small strains. The temperature of the bottom plate is gradually increased from ambient to 120 °C over a duration of 30 min.

Dewetting Experiments. For the dewetting experiments, the substrates used had grating geometry; were prepared with a CD stamp, and had feature height varying from 115 nm at one end to 11 nm on the other end, over a distance of 35 mm. The width of the substrate was 25 mm. On these substrates, thin Polystyrene films (MW: 280 K, Sigma, UK) directly spin coated from a dilute solution (c_n = 1.25%) in HPLC grade toluene (SRL Chemicals, India). The dispensed drop volume was 400 μL, RPM 2500, and duration of spinning was 1 min. After spin coating, the films were air annealed at room temperature for 1 h and subsequently at 60 °C for 6 h in a vacuum oven to remove any residual solvent. Before dewetting, the as cast morphology of the film was investigated using an AFM, at different locations of the substrate. In

dx.doi.org/10.1021/am500163s | ACS Appl. Mater. Interfaces 2014, 6, 6579−6588

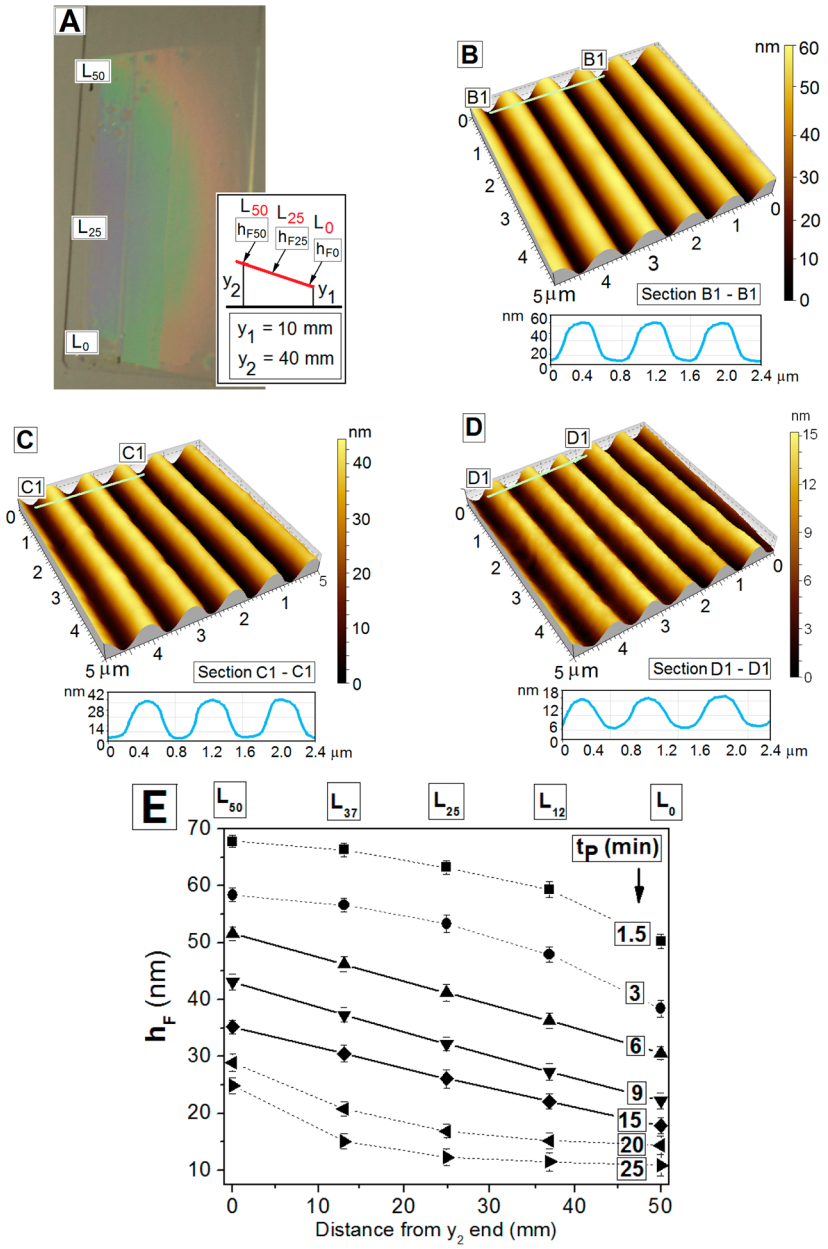

Figure 2. (A) Digicam image of a topographic gradient with continuous variation in feature height. The diffraction color confirms the presence of the patterns over the entire surface. The locations where the AFM scans have been performed are marked. Inset shows the experimental arrangement. (B–D) AFM scan of the film surface at locations L_{50}, L_{25}, and L_0, respectively, where the suffix of L indicates the distance of the location in mm from the y_1 end of the film. (E) Spatial variation of feature height at different locations of the film as a function of precuring time (t_P) for y_1 = 10 mm and y_2 = 40 mm.

some samples, part of the film was deliberately removed to measure the exact feature height at that location (example shown in Figure 6A). The films were thermally dewetted by annealing them at 130 °C for different durations in a vacuum oven. The samples were withdrawn from the oven, cooled to room temperature, and were morphologically characterized using an optical microscope (Leica, DMLM 2500) and an AFM.

Films directly coated on a topographically patterned substrate have undulating top surfaces and therefore are defined in terms of equivalent thickness (h_E), which is the thickness of a film coated under identical condition on a flat substrate of the same material.[57] The equivalent thickness of films used in this study includes h_E = 51.3 ± 1.1 nm. The film thickness on flat cross-linked Sylgard 184 substrates were measured using an imaging Ellipsometer (Accuron GmbH, model EP3). A detailed parametric variation for different equivalent film thickness is beyond the scope of this study and will be taken up separately.

RESULTS AND DISCUSSIONS

Figure 2A shows a digital camera image of a 5 μm thick patterned film which has continuous variation in feature height (h_F) along its length. A DVD foil (h_0 = 75 nm) is used as the stamp. The existence of the patterns over the entire surface can be ascertained from the appearance of rainbow colors arising out of optical diffraction.[54] For the specific sample shown in Figure 2A, the height of the spacer blocks are 10 mm (y_1) and 40 mm (y_2) respectively and t_P = 6 min. The morphology of the patterns at locations L_{50}, L_{25}, and L_0 are shown in Figure 2B–D, respectively. The feature heights at different locations of the samples are found to be h_{F0} = 30.6 ± 0.6 nm, h_{F12} = 36.3 ± 0.4 nm, h_{F25} = 41.2 ± 0.5 nm, h_{F37} = 46.2 ± 0.3 nm, and h_{F50} = 51.6 ± 0.4 nm. In Figure 2E, it can be seen that the variation of h_F along L is nearly linear for t_P = 6 min. Other data sets in the same figure

dx.doi.org/10.1021/am500163s | ACS Appl. Mater. Interfaces 2014, 6, 6579–6588

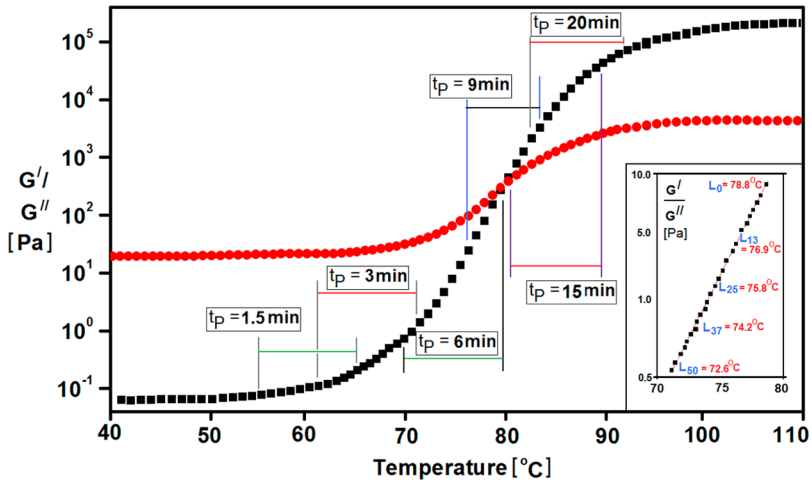

Figure 3. Variation in storage modulus (G') and loss modulus (G'') with progressive annealing, as measured using a plate and cone Rheometer having plate diameter of 25 mm, cone angle of 2°, and sample thickness ∼1 mm, under controlled shear stress condition at a constant angular frequency of 10 s^{-1} and a strain amplitude of 5%. Inset shows the detailed variation in G' with L for the sample for t_P = 6 min.

corresponding to different durations of t_P shows that the steepness of the gradient as well as the maximum and minimum h_F at the two ends of the sample depends on t_P. Also, at any specific location, h_F progressively reduces with longer precuring. Additionally, we observe that the variation of h_F with L is almost linear for intermediate values of t_P ranging between 6 to 15 min (shown with bold connecting lines). For lower (1.5 and 3 min) and higher (20 and 25 min) t_P, the variation is not linear. Similar dependence of h_F with L as a function of t_P is also observed for other combinations of y_1 and y_2, which can be seen in Figure S1 in the Supporting Information. This allows controlling the steepness of the gradient.

During precuring, the temperature at any point on the film surface depends on the rate of heat transferred between that specific point and the heat source. Because of the slanted orientation of the film with respect to the heat source, the total heat flux (Q_T) varies along L. To have a quantitative estimate of the temperature gradient generated across the film surface, we conduct a heat flux analysis (shown in the Supporting Information). The analysis reveals that both convection and radiation contributes in the heat transfer between hot plate and the film. The convective part of the heat transfer can be fairly assumed because of the air flow between the plate and the film mounting (that is flow between AD and BC as shown in Figure S2.1 of the Supporting Information). It is worth highlighting that the radiative heat flux (Q_R) is not negligible and is almost 10% of the convective heat flux (Q_C) in terms of magnitude. Q_T is maximum at the y_1 end and gradually reduces toward the y_2 end as the separation distance between the hot plate and the film surface increases. This results in a continuous variation in the surface temperature (T_S) along the length of the film.

For a methyl-vinly (poly)dimethylsiloxane as in the case of Sylgard 184, the cross-linking reaction follows the mechanism of macro free-radical coupling. The forward and backward conversion during the decomposition of the curing agent to form free-radicals can be denoted by half-time at a particular temperature. The half-time temperature relation in this case can be expressed by the classical Arrhenius relation[58]

$$k_d = A_0 \exp(-E_a/RT) \text{ and } t_{1/2} = \frac{0.693}{k_d} \quad (1)$$

In the above expression, k_d is the rate constant, A_0 is the frequency factor. From this equation it becomes clear that the rate of generation of free-radicals maximizes at elevated temperatures, which in turn enhances the rate of the cross-linking of PDMS in areas of the film which receive higher Q_T vis-a-vis have higher surface temperature. It should however be noted that in case of vinyl terminated (poly)dimethylsiloxane, at very high temperature, an effect called "scorching" may take place, which may delay the cross-linking reaction.[59] Hence, the temperature regulation at the surface of films becomes very important.

Figure 3 indicates the variation of viscoelastic modulii of a Sylgard 184 film as a function of temperature. As there is continuous variation of temperature along the film surface during precuring, part of the curve that covers the temperature range prevailing between the two ends of the film surface essentially captures the spatial variation in the rheological properties along the length of the film at the time of imprinting. During imprinting the film, part of the externally applied energy gets stored within the film (component E_E) as elastic deformation of the partially cross-linked elastomer, while the remaining part of energy (component E_V) is lost due viscous dissipation.[60] The existing viscoelasticity gradient within the film after precuring results in different relative magnitudes of E_E and E_V along L. The magnitude of E_E depends on the storage modulus (G') which is maximum at y_1 end of the film, as T_s is maximum there. As temperature progressively reduces from y_1 to y_2 end of the film, G' also reduces in the same direction. Once the external pressure is withdrawn, the polymer film which is in a nonequilibrium state exhibits partial relaxation of the accumulated stresses which in turn results in partial flattening of the imprinted film surface. The magnitude of feature height reduction (h_{RED}) at any location depends on the local magnitude of G'. As G' gradually decreases from y_1 to y_2, h_{RED} also reduces along that direction. Consequently, the final feature height ($h_F = h_0 - h_{RED}$) gradually increases from y_1 to y_2 resulting in a gradient topography. The presence of the stamp on the film surface, even after the external load has been withdrawn ensures that the imprinted structures cannot dilate laterally during the surface flattening process and periodicity of the patterns remain unaltered to that of the stamp. As G' (and consequently, E_E) at any specific location increases with t_P, the magnitude of h_{RED} at that location also increases with

dx.doi.org/10.1021/am500163s | ACS Appl. Mater. Interfaces 2014, 6, 6579−6588

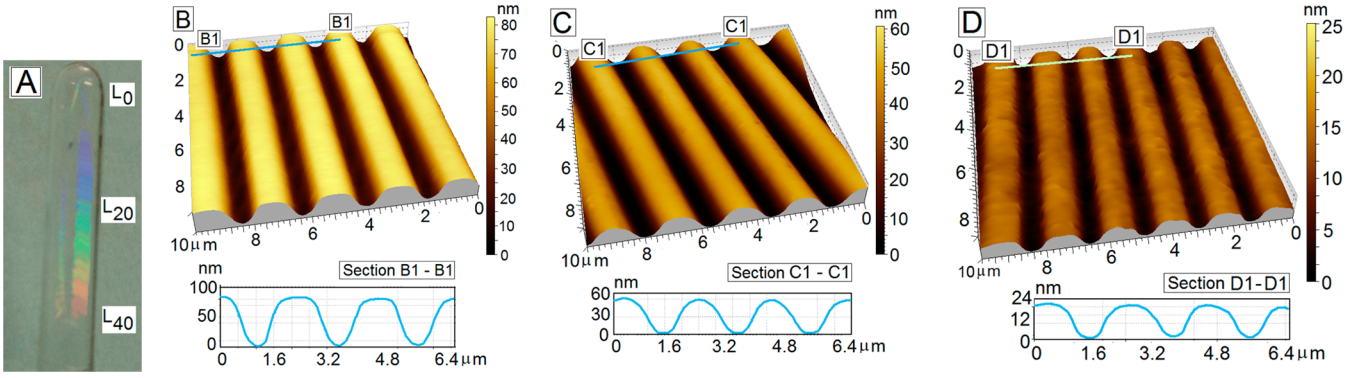

Figure 4. (A) Digicam image of a film with topographic gradient coated on a cylindrical glass tube. The diffraction color confirms the presence of the patterns over the entire surface. The locations where the AFM scans have been performed are marked. (B–D) AFM scans of the patterns along with cross-sectional line profile at locations L_{40}, L_{20}, and L_0 respectively. The suffix of L indicates the distance of the location in mm from the y_1 end of the film. For the specific experiment, t_P = 12 min, y_1 = 0 mm, and y_2 = 30 mm.

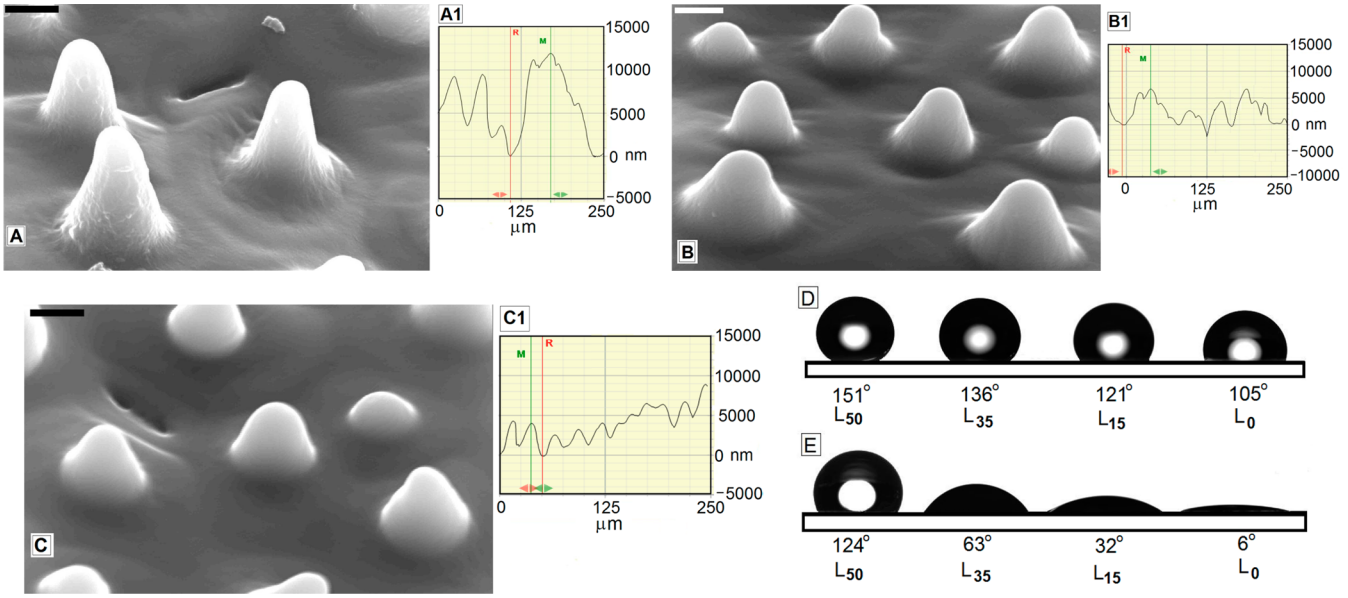

Figure 5. (A–C) SEM image (secondary electron image showing topographic contrast) of patterns obtained on the surface of a film at L_{50}, L_{37}, and L_{12} with a biomimetic stamp. The inset shows the corresponding profilometer scans. The scale bars correspond to 5 μm. (D, E) Equilibrium contact angle with water at different locations on a gradient PDMS film and a UVO treated PDMS film, respectively, created with a biomimetic stamp.

longer t_P, resulting in lowering of h_F (Figure 2E). Figure 2E also reveals that the variation of h_F along L exhibits different trends with change in t_P. The variation is found to be linear only for certain intermediate values of t_P and is nonlinear when t_P is either very low or very high. A similar trend is observed for other combinations of y_1 and y_2 as well, which can be seen in Figure S1 in the the Supporting Information. To understand this occurrence, we look at the measured values of surface temperature (T_S) at different locations of the film. For the particular sample shown in Figure 2A (t_P = 6 min, y_1 =10 mm, and y_2 = 40 mm), the values of T_S at different locations are T_{S-L0} = 78.8 °C, T_{S-L13} = 76.9 °C, T_{S-L25} = 75.8 °C, T_{S-L37} = 74.2 °C and T_{S-L50} = 72.5 °C. This temperature range is marked on the modulus plot (Figure 3) and it is observed that within this range, the variation of G' with T is linear (inset of Figure 3). This implies that the spatial variation of G' along the film surface is linear, which results in a linear variation of h_{RED} along L. This explains the observed linear variation of h_F (= $h_0 - h_{RED}$; h_0 is constant) along L. The measured range of temperature variation over the film surface for different durations of t_P is also marked on Figure 3. It can be seen that the variation in G' with T (and hence, along L) is linear only for t_P = 6, 9, and 15 min, which explains the linear variation of h_F with L for these intermediate durations of t_P. For low (t_P = 1.5 and 3 min) and high (t_P = 20 and 25 min), the variation of G' with T is nonlinear, which is reflected as non linear variation of h_F with L in Figure 2E. Enhancement of the externally applied stress during imprinting has no effect on h_F, as E_E depends on the extent of cross-linking of the film, and therefore any additional energy augments to the E_V component and gets dissipated.

The digicam image in Figure 4A shows that a topographic gradient surface has also been created on a film coated on a cylindrical substrate. In the specific example, y_1 is 0 mm, y_2 = 30 mm, t_P = 12 min and CD foil with h_P of ~120 nm is used as the stamp. The AFM images 4B–D shows that the final depth of the features (h_F) varies from 23.2 nm at the y_1 end to ~81.3 nm at the y_2 end. The tube is manually rotated during precuring to maintain radial temperature uniformity as well as manually rolled over the stamp during attachment of it on to the partially cured film and to ensure uniform pressure along the entire circumference.

dx.doi.org/10.1021/am500163s | ACS Appl. Mater. Interfaces 2014, 6, 6579–6588

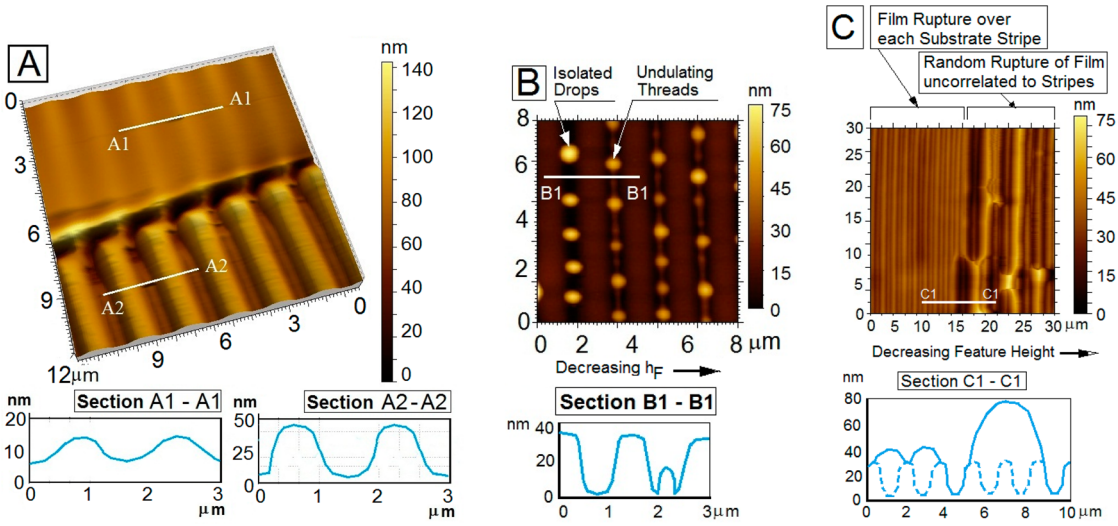

Figure 6. (A) AFM image of an area where the as cast PS film on the gradient topography substrate has been partially removed to uncover the underlying substrate. The sections show the amplitude of the as cast film and the local feature height of the substrate. (B) Morphological regime cross over from array of aligned isolated droplet to aligned undulating threads for h_{FC1} = 38.6 nm. (C) Second morphological regime cross over and ordered to disordered transition for h_{FC2} = 21.4 nm. The film is seen to rupture over each substrate stripe on the left side and with the formation of nucleated holes uncorrelated to substrate patterns on the right side. For all the frames, h_E = 51.3 nm.

However, we must admit that this approach is valid only as a proof of concept, and any practical implementation would require automated rotation of the cylindrical substrate.

We observe that there is hardly any wettability gradient in any of the topographic gradient surfaces fabricated using CD/DVD stamps along their length. This is attributed to the low aspect ratio of the CD/DVD stamps, and consequently the wetting regime over the entire surface remains in the Wenzel state. To demonstrate the utility of the proposed method in generating a gradient wettability surface, we used biomimetic stamps with higher levels of roughness.[52] The morphology of the imprinted features obtained at different locations on a 20 μm thick film, for t_P = 7 min, y_1 = 0 and y_2 = 30 mm is shown in Figure 5A–C. Complementary analysis with surface profilometer shows that the RMS roughness of the films drops from ~14.23 μm at L_{50} to ~4.39 μm at L_{13} (shown as insets), and down to <400 nm at L_0. Figure 5D shows that the gradient in feature height (or roughness) obtained using a negative replica of a lotus leaf as stamp results in progressive variation of water contact angle from 156° at L_{50} down to 103° at L_0. The only limitation of this wettability gradient surface is that the entire variation of WCA is confined within the hydrophobic regime (θ_E > 103°), as a flat cross-linked Sylgard 184 film surface itself has $\theta_E \approx 100°$. A more versatile wettability gradient surface that exhibits WCA variation all the way from complete wetting at one end to hydrophobicity at the other end is obtained by exposing the surface (shown in Figure 5D) to UV–ozone for 30 min. As discussed in details earlier, the UV exposure of Sylgard 184 film in the presence of oxygen and ozone results in the formation of a hydrophilic surface oxide layer. Consequently the variation of θ_E changes from near complete wetting at $\mathbf{y_1}$ to significant level of hydrophobicity (WCA ~ 124°) at the y_2 end. We would like to highlight that though we could successfully create a surface with significant wettability gradient, no movement of water drop along the surface due to a passive wettability gradient was observed. We feel this is due to strong pinning of the contact line on a soft surface where the vertical component of liquid surface tension ($\gamma_L \sin\theta$) may result in an intrinsic local deformation on the elastomeric film, enhancing the pinning of the three phase contact line. Lastly, we would also like to highlight that the proposed method is in no way limited to the use of a biomimetic stamp, and can be implemented with any lithographically fabricated master as well.

Application of the Gradient Surfaces: Combinatorial Dewetting studies. In this section we highlight some possible applications of the topographic gradient surfaces created by the proposed technique. We used the gradient surfaces with regular features to study the influence of substrate feature height (h_F) on dewetting of ultrathin (h < 100 nm) polymer films. It is known that the morphology of the patterns arising out of dewetting of a thin polymer film on a topographically patterned substrate depends on h_F.[48] Typically, on a grating patterned substrate the dewetted morphology changes from an array of aligned droplets to undulating threads and eventually to large, random dewetted droplets uncorrelated to the substrate patterns, with progressive reduction in h_F. However, as separate samples for each h_F were used in the earlier studies, the exact critical feature height (h_{FC}) at which the morphology changes from one regime to the other was not possible to identify. Additionally, there is always a slight variation of film thickness in each sample, which may be critical for ultrathin films and might give rise to erroneous observations. We show that these limitations can be overcome when a gradient topography substrate is used for studying dewetting. It is worth highlighting that though such combinatorial dewetting studies have been reported on a chemically gradient substrate before,[61] no such study on a topographically patterned substrate is available in the literature. Almost all parametric studies on topographic pattern directed dewetting of thin polymer films has been performed on substrates with fixed feature height.[62]

Figure 6A is a unique image, where part of the as cast film has been deliberately removed following protocol discussed elsewhere,[57] which allows determining the exact amplitude of the undulating film surface as well as the exact local h_F. For the specific image shown in Figure 6A, h_F = 46.4 nm, and the local amplitude of the continuous film on the substrate is ≈11.4 nm, which can be seen clearly from the cross sectional line scans provided in insets 6A1 and 6A2 respectively. As already mentioned in the experimental section, for all the dewetting

dx.doi.org/10.1021/am500163s | ACS Appl. Mater. Interfaces 2014, 6, 6579–6588

experiments, h_E was maintained at 51.3 nm. Panels B and C in Figure 6 shows different morphological regime cross overs and allows us to determine h_{FC} accurately. In Figure 6B, it can be seen that when h_F = 38.6 nm, the morphology of the dewetted droplets changes from isolated aligned drops (left part of the image) to ordered undulating threads confined within the substrate grooves (right part of the image). The reason for the suppression of droplet formation is attributed to complete filling of the substrate grooves by the polymer threads, which laterally confines the growth of Rayleigh Instability mediated disintegration of the threads in to droplets. Further reduction of the feature height lead to another kind of morphological regime cross over, which can be seen in Figure 6C, for h_F = 21.4 nm. It can be seen on the left side of the figure that the film ruptures over each substrate stripe, where the film thickness is thinnest. On the other hand, on the right side of the figure it is noted that the film has ruptured with the formation of nucleated holes which are not fully correlated to the substrate features, though the rims of the growing holes are still seen to be aligned along the substrate patterns. Thus, it can argued that for h_F < 21.4 nm, there is a critical ordered to disordered transition in dewetting of a thin film on a grating patterned substrate. However, it must be noted that the values of h_{FC1} = 38.6 nm and h_{FC2} = 21.4 nm are valid only for h_E = 51.3 nm and on a specific substrate with λ_P =1.5 μm and l_P = 750 nm. A detailed parametric variation involving h_E, λ_P, l_P, the steepness of the gradient and the substrate geometry is beyond the scope of this paper and will be taken up separately. However, panels B and C in Figure 6 show that the topographic gradient substrates created by the proposed method can be used for performing combinatorial studies related to pattern directed dewetting and can also be unambiguously used to find out the critical values of h_{FC} at which morphological regime cross over takes place.

The biomimetic gradient surfaces can also find potential application in various types of combinatorial studies. For example, recently we have studied the flow behavior in a micro fluidic channel where one side was superhydrophobic and was fabricated by double replication of a lotus leaf on cross-linked Sylgard 184.[55] It was observed that depending on the micro confinement effect, there can be two flow regimes, even at low Reynolds number. The first regime is characterized by an apparent slip-stick flow, that results in an enhanced bulk throughput. In contrast, the second regime exhibits a complete breakdown of the laminar, uniaxial flow model and leads to predominantly no-slip flow. If a micro channel can be fabricated on the biomimetic gradient surfaces, we feel that the flow regime cross over as a function of the roughness of the wall can be shown in greater detail. It will also be possible to capture the precise location along the flow path (under a microscope) where the regime cross over takes place and to track the change in the flow patterns in situ. The work is presently underway.

CONCLUSIONS

In this paper, we have reported a simple yet novel method for creating a gradient topography surface on an elastomeric thin film, in which the feature height (h_F) varies continuously along the length of the film, while the line width and periodicity of the features remains the same across the entire surface. The method relies on introducing a pre-existing gradient in cross-link density over the surface to be imprinted by tailoring the rate of cross-linking reaction by means of a temperature gradient. This introduces a spatial variation in viscoelasticity over the film. The precured film, when imprinted under an intermittent applied stress, relaxes partially based on the storage and loss moduli at each point. The manifestation of the stress relaxation is partial flattening of the imprinted film surface during which the preexisting viscoelasticity gradient leads to differential rates of surface flattening, resulting in the gradient topography. The proposed technique, which combines essential elements of soft lithography, polymer cross-linking and control over thermal processes in a interesting new platform. The utility of the proposed technique lies in the fact that the procedure is simple, versatile, employs commercially available materials, does not require any sophisticated instruments, and hence may be replicated easily by other researchers for their specific applications. The method is capable of generating the topography gradient in a single step, which is in clear contrast to most other previously reported methods which either involve multiple processing steps including the use of a chemically gradient template or expensive custom tailored masks with spatially varying feature dimension. We have also shown that the nature of variation of h_F with L as well as the steepness of the gradient can be controlled by controlling the various processing conditions. The simplicity of the method makes it implementable without any specialized fabrication facility and is thus is particularly attractive for researchers who are non expert in the field of nano fabrication, but require topographic gradient surfaces as templates for various combinatorial experiments.

The use of a flexible stamp enables us to extend the technique for creating a topographic gradient on a film coated on a non planar surface as well, which is yet another novel aspect of this work. Finally, we have also shown that by using high aspect ratio biomimetic stamps, it is possible to create surfaces with significant wettability gradient, spanning between complete wetting at one end to significant level of hydrophobicity (~125°) at the other end of the film.

We have also shown that performing combinatorial dewetting experiments on the gradient surfaces can be used to unambiguously determine the critical substrate feature height (h_{FC}) at which the arrangement of the dewetted patterns change from one morphological regime to the other.

ASSOCIATED CONTENT

Supporting Information

The variation of the steepness of the gradient as a function of y_1 and y_2 for different extents of precuring (Figure S1) and simulations of temperature gradient over the film surface to calculate the heat flux, including the contribution of radiation (Figures S2.1−S2.5). This material is available free of charge via the Internet at http://pubs.acs.org/.

AUTHOR INFORMATION

Corresponding Author

*E-mail: rabibrata@che.iitkgp.ernet.in. Tel:+91-3222 283912.

Author Contributions

†Authors S.R. and N.B. contributed equally to this work.

Notes

The authors declare no competing financial interest.

ACKNOWLEDGMENTS

R.M. acknowledges the support of the Department of Science & Technology (DST), New Delhi, Government of India, for funding the research under its Nano Mission program (SR/NM/NS-63/2010). The authors also acknowledge Prof. P. K. Das of Mechanical Engineering Department, IIT Kharagpur, for helping

them with the heat transfer calculations and other useful discussions.

REFERENCES

(1) Luo, W.; Yousaf, M. N. Tissue Morphing Control on Dynamic Gradient Surfaces. *J. Am. Chem. Soc.* **2011**, *133*, 10780−10783.
(2) Elwing, H.; Golander, C. G. Protein and Detergent Interaction Phenomena on Solid Surfaces with Gradient in Chemical Composition. *Adv. Colloid Interface Sci.* **1990**, *32*, 317−339.
(3) Gunawan, R. C.; Silvestre, J. H.; Gaskins, R.; Kenis, P. J. A.; Leckband, D. E. Cell Migration and Polarity on Microfabricated Gradients of Extracellular Matrix Proteins. *Langmuir* **2006**, *22*, 4250−4258.
(4) Chang, T.; Rozkiewicz, D. I.; Ravoo, B. J.; Meijer, E. W.; Reinhoudt, D. N. Directional Movement of Dendritic Macromolecules on Gradient Surfaces. *Nano Lett.* **2007**, *7*, 978−980.
(5) Li, J.; Han, Y. Optical Intensity Gradient by Colloidal Photonic Crystals with a Graded Thickness Distribution. *Langmuir* **2006**, *22*, 1885−1890.
(6) Kim, M. S.; Khang, G.; Lee, H. B. Gradient Polymer Surfaces for Biomedical Applications. *Prog. Polym. Sci.* **2008**, *33*, 138−164.
(7) Potyrailo, R. A.; Hassib, L. Analytical Instrumentation Infrastructure for Combinatorial and High-throughput Development of Formulated Discrete and Gradient Polymeric Sensor Materials Arrays. *Rev. Sci. Instrum.* **2005**, *76*, 062225.
(8) Roberson, S. V.; Fahey, A. J.; Sehgal, A.; Karim, A. Multifunctional ToF-SIMS: Combinatorial Mapping of Gradient Energy Substrates. *Appl. Surf. Sci.* **2002**, *200*, 150−164.
(9) Meredith, J. C.; Smith, A. P.; Karim, A.; Amis, E. J. Combinatorial Materials Science for Polymer Thin-Film Dewetting. *Macromolecules* **2000**, *33*, 9747−9756.
(10) Ashley, K. M.; Meredith, J. C.; Amis, E.; Raghavan, D.; Karim, A. Combinatorial Investigation of Dewetting: Polystyrene Thin Films on Gradient Hydrophilic Surfaces. *Polymer* **2003**, *44*, 769−772.
(11) Julthongpiput, D.; Fasolka, M. J.; Zhang, W.; Nguyen, T.; Amis, E. J. Gradient Chemical Micropatterns: A Reference Substrate for Surface Nanometrology. *Nano Lett.* **2005**, *5*, 1535−1540.
(12) Julthongpiput, D.; Zhang, W.; Douglas, J. F.; Karim, A.; Fasolka, M. J. Pattern-directed to Isotropic Dewetting Transition in Polymer Films on Micropatterned Surfaces with Differential Surface Energy Contrast. *Soft Matter* **2007**, *3*, 613−618.
(13) Roy, S.; Mukherjee, R. Ordered to Isotropic Morphology Transition in Pattern-Directed Dewetting of Polymer Thin Films on Substrates with Different Feature Heights. *ACS Appl. Mater. Interfaces* **2012**, *4*, 5375−5385.
(14) Chaudhury, M. K.; Whitesides, G. M. How to Make Water Run Uphill. *Science* **1992**, *256*, 1539−1541.
(15) Bain, C. D.; Burnett-Hall, G. D.; Montgomerie, R. R. Rapid Motion of Liquid Drops. *Nature* **1994**, *372*, 414−415.
(16) Daniel, S.; Chaudhury, M. K.; Chen, J. C. Fast Drop Movements Resulting from the Phase Change on a Gradient Surface. *Science* **2001**, *291*, 633−636.
(17) Shastry, A.; Case, M. J.; Böhringer, K. F. Directing Droplets Using Microstructured Surfaces. *Langmuir* **2006**, *22*, 6161−6167.
(18) Ito, Y.; Heydari, M.; Hashimoto, A.; Konno, T.; Hirasawa, A.; Hori, S.; Kurita, K.; Nakajima, A. The Movement of a Water Droplet on a Gradient Surface Prepared by Photodegradation. *Langmuir* **2007**, *23*, 1845−1850.
(19) Reyssat, M.; Pardo, F.; Quéré, D. Drops Onto Gradients of Texture. *Europhys. Lett.* **2009**, *87*, 36003.
(20) Das, A. K.; Das, P. K. Multimode Dynamics of a Liquid Drop over an Inclined Surface with a Wettability Gradient. *Langmuir* **2010**, *26*, 9547−9555.
(21) Morgenthaler, S.; Zink, C.; Spencer, N. D. Surface-Chemical and -Morphological Gradients. *Soft Matter* **2008**, *4*, 419−434.
(22) Elwing, H.; Welin, S.; Askendal, A.; Nilsson, U.; Lundström, I. A Wettability Gradient Method for Studies of Macromolecular Interactions at the Liquid/Solid Interface. *J. Colloid Interface Sci.* **1987**, *119*, 203−210.
(23) Yu, X.; Wang, Z.; Jiang, Y.; Zhang, X. Surface Gradient Material: From Superhydrophobicity to Superhydrophilicity. *Langmuir* **2006**, *22*, 4483−4486.
(24) Beurer, E.; Venkataraman, N. V.; Rossi, A.; Bachmann, F.; Engeli, R.; Spencer, N. D. Orthogonal, Three-Component, Alkanethiol-Based Surface-Chemical Gradients on Gold. *Langmuir* **2010**, *26*, 8392−8399.
(25) Liedberg, B.; Tengvall, P. Molecular Gradients of ω-Substituted Alkanethiols on Gold: Preparation and Characterization. *Langmuir* **1995**, *11*, 3821−3827.
(26) Choi, S. H.; Newby, B. Z. Micrometer-Scaled Gradient Surfaces Generated Using Contact Printing of Octadecyltrichlorosilane. *Langmuir* **2003**, *19*, 7427−7435.
(27) Ionov, L.; Sidorenko, A.; Stamm, M.; Minko, S.; Zdyrko, B.; Klep, V.; Luzinov, I. Gradient Mixed Brushes: "Grafting To" Approach. *Macromolecules* **2004**, *37*, 7421−7423.
(28) Fuierer, R. R.; Carroll, R. L.; Feldheim, D. L.; Gorman, C. B. Patterning Mesoscale Gradient Structures with Self-Assembled Monolayers and Scanning Tunneling Microscopy Based Replacement Lithography. *Adv. Mater.* **2002**, *14*, 154−157.
(29) Zhang, S.; You, B.; Gu, G.; Wu, L. A Simple Approach to Fabricate Morphological Gradient on Polymer Surfaces. *Polymer* **2009**, *50*, 6235−6244.
(30) Bhat, R. R.; Fischer, D. A.; Genzer, J. Fabricating Planar Nanoparticle Assemblies with Number Density Gradients. *Langmuir* **2002**, *18*, 5640−5643.
(31) Bhat, R. R.; Genzer, J.; Chaney, B. N.; Sugg, H. W.; Liebmann-Vinson, A. Controlling the Assembly of Nanoparticles using Surface Grafted Molecular and Macromolecular Gradients. *Nanotechnology* **2003**, *14*, 1145−1152.
(32) Huwiler, C.; Kunzler, T. P.; Textor, M.; Vörös, J.; Spencer, N. D. Functionalizable Nanomorphology Gradients via Colloidal Self-Assembly. *Langmuir* **2007**, *23*, 5929−5935.
(33) Zhang, J.; Xue, L.; Han, Y. Fabrication of Gradient Colloidal Topography. *Langmuir* **2005**, *21*, 5667−5671.
(34) Zhang, J.; Xue, L.; Han, Y. Fabrication Gradient Surfaces by Changing Polystyrene Microsphere Topography. *Langmuir* **2005**, *21*, 5−8.
(35) Stafford, C. M.; Roskov, K. E.; Epps, T. H., III; Fasolka, M. J. Generating Thickness Gradients of Thin Polymer Films via Flow Coating. *Rev. Sci. Instrum.* **2006**, *77*, 023908.
(36) Tsai, I. Y.; Kimura, M.; Russell, T. P. Fabrication of a Gradient Heterogeneous Surface Using Homopolymers and Diblock Copolymers. *Langmuir* **2004**, *20*, 5952−5957.
(37) Smith, A. P.; Douglas, J. F.; Meredith, J. C.; Amis, E. J.; Karim, A. Combinatorial Study of Surface Pattern Formation in Thin Block Copolymer Films. *Phys. Rev. Lett.* **2001**, *87*, 015503.
(38) Zhang, J.; Han, Y. A Topography/Chemical Composition Gradient Polystyrene Surface: Toward the Investigation of the Relationship between Surface Wettability and Surface Structure and Chemical Composition. *Langmuir* **2008**, *24*, 796−801.
(39) Genzer, J.; Fischer, D. A.; Efimenko, K. Combinatorial Near-edge X-ray Absorption Fine Structure: Simultaneous Determination of Molecular Orientation and Bond Concentration on Chemically Heterogeneous Surfaces. *Appl. Phys. Lett.* **2003**, *82*, 266−268.
(40) Lee, J. H.; Kim, H. G.; Khang, G. S.; Lee, H. B.; Jhon, M. S. Characterization of Wettability Gradient Surfaces Prepared by Corona Discharge Treatment. *J. Colloid Interface Sci.* **1992**, *151*, 563−570.
(41) Sun, C.; Zhao, X. W.; Han, Y. H.; Gu, Z. Z. Control of Water Droplet Motion by Alteration of Roughness Gradient on Silicon Wafer by Laser Surface Treatment. *Thin Solid Films* **2008**, *516*, 4059−4063.
(42) Pitt, W. G. Fabrication of a Continuous Wettability Gradient by Radio Frequency Plasma Discharge. *J. Colloid Interface Sci.* **1989**, *133*, 223−227.
(43) Cao, H.; Tegenfeldt, J. O.; Austin, R. H.; Chou, S. Y. Gradient Nanostructures for Interfacing Microfluidics and Nanofluidics. *Appl. Phys. Lett.* **2002**, *81*, 3058−3060.
(44) Long, C. J.; Schumacher, J. F.; Brennan, A. B. Potential for Tunable Static and Dynamic Contact Angle Anisotropy on Gradient Microscale Patterned Topographies. *Langmuir* **2009**, *25*, 12982−12989.

(45) Kumar, T. A.; Bardea, A.; Shai, Y.; Yoffe, A.; Naaman, R. Patterning Gradient Properties from Sub-Micrometers to Millimeters by Magnetolithography. *Nano Lett.* **2010**, *10*, 2262−2267.
(46) Langley, K. R.; Sharp, J. S. Microtextured Surfaces with Gradient Wetting Properties. *Langmuir* **2010**, *26*, 18349−18356.
(47) Ding, Y.; Qi, H. J.; Alvine, K. J.; Ro, H. W.; Ahn, D. U.; Lin-Gibson, S.; Douglas, J. F.; Soles, C. L. Stability and Surface Topography Evolution in Nanoimprinted Polymer Patterns under a Thermal Gradient. *Macromolecules* **2010**, *43*, 8191−8201.
(48) Roy, S.; Mukherjee, R. Ordered to Isotropic Morphology Transition in Pattern-Directed Dewetting of Polymer Thin Films on Substrates with Different Feature Heights. *ACS Appl. Mater. Interfaces* **2012**, *4*, 5375−5385.
(49) Gentili, D.; Foschi, G.; Valle, F.; Vavallini, M.; Biscarini, F. Applications of Dewetting in Micro and Nanotechnology. *Chem. Soc. Rev.* **2012**, *41*, 4430−4443.
(50) Sylgard 184 Product Data (http://www3.dowcorning.com/DataFiles/090007b281eb2ada.pdf).
(51) Mukherjee, R.; Sharma, A. Creating Self-Organized Submicrometer Contact Instability Patterns in Soft Elastic Bilayers with a Topographically Patterned Stamp. *ACS Appl. Mater. Interfaces* **2012**, *4*, 355−362.
(52) Mukherjee, R.; Sharma, A.; Gonuguntla, M.; Patil, G. K. Adhesive Force Assisted Imprinting of Soft Solid Polymer Films by Flexible Foils. *J. Nanosci. Nanotechnol.* **2008**, *8*, 3406−3415.
(53) Das, A. L.; Mukherjee, R.; Katiyer, V.; Kulkarni, M.; Ghatak, A.; Sharma, A. Generation of Sub-micrometer-scale Patterns by Successive Miniaturization Using Hydrogels. *Adv. Mater.* **2007**, *19*, 1943−1946.
(54) Cassie, A. B. D.; Baxter, S. Wettability of Porous Surfaces. *Trans. Faraday Soc.* **1944**, *40*, 546−551.
(55) Dey, R.; Raj, K. M.; Bhandaru, N.; Mukherjee, R.; Chakraborty, S. Tunable Hydrodynamic Characteristics in Microchannels with Biomimetic Superhydrophobic (Lotus Leaf Replica) Walls, *Soft Matter* **2014**, DOI:10.1039/c4sm00037d.
(56) Mukherjee, R.; Patil, G. K.; Sharma, A. Solvent Vapor-Assisted Imprinting of Polymer Films Coated on Curved Surfaces with Flexible PVA Stamps. *Ind. Eng. Chem. Res.* **2009**, *48*, 8812−8818.
(57) Roy, S.; Ansari, K. J.; Jampa, S. S. K.; Vutukuri, P.; Mukherjee, R. Influence of Substrate Wettability on the Morphology of Thin Polymer Films Spin-Coated on Topographically Patterned Substrates. *ACS Appl. Mater. Interfaces* **2012**, *4*, 1887.
(58) Msakni, A.; Chaumont, P.; Cassagnau, P. Diffusion of the Dicumyl Peroxide in Molten Polymer Probed by Rheology. *Rheol. Acta* **2007**, *46*, 933−943.
(59) Dorn, M. Modification of Molecular Weight and Flow Properties of Thermoplastics. *Adv. Polym. Technol.* **1985**, *5*, 87−97.
(60) Bhandaru, N.; Roy, S.; Suruchi; Harikrishnan, G.; Mukherjee, R. Lithographic Tuning of Polymeric Thin Film Surfaces by Stress Relaxation. *ACS Macro Lett.* **2013**, *2*, 195−200.
(61) Julthongpiput, D.; Zhang, W.; Douglas, J. F.; Karim, A.; Fasolka, M. J. Pattern-directed to Isotropic Dewetting Transition in Polymer Films on Micropatterned Surfaces with Differential Surface Energy Contrast. *Soft Matter* **2007**, *3*, 613−618.
(62) Mukherjee, R.; Bandyopadhyay, D.; Sharma, A. Control of Morphology in Pattern Directed Dewetting of Thin Polymer Films. *Soft Matter* **2008**, *4*, 2086−2097.